

# UV Irradiation of Polycyclic Aromatic Hydrocarbons in Ices: Production of Alcohols, Quinones, and Ethers

Max P. Bernstein,<sup>1,2\*</sup> Scott A. Sandford,<sup>1</sup> Louis J. Allamandola,<sup>1</sup> J. Seb Gillette,<sup>3</sup> Simon J. Clemett,<sup>3</sup> Richard N. Zare<sup>3</sup>

Polycyclic aromatic hydrocarbons (PAHs) in water ice were exposed to ultraviolet (UV) radiation under astrophysical conditions, and the products were analyzed by infrared spectroscopy and mass spectrometry. Peripheral carbon atoms were oxidized, producing aromatic alcohols, ketones, and ethers, and reduced, producing partially hydrogenated aromatic hydrocarbons, molecules that account for the interstellar 3.4-micrometer emission feature. These classes of compounds are all present in carbonaceous meteorites. Hydrogen and deuterium atoms exchange readily between the PAHs and the ice, which may explain the deuterium enrichments found in certain meteoritic molecules. This work has important implications for extraterrestrial organics in biogenesis.

Infrared (IR) spectroscopy of the interstellar medium (ISM), combined with laboratory studies of realistic interstellar analog materials, is a powerful means for identifying the matter that exists between the stars. The ISM is known to contain a variety of grains, including silicates, carbon-rich particles, and ices (1), and a large number of gas-phase species (2). The most abundant and widespread class of carbon-carrying gaseous species is believed to be PAHs (3–5). In dense molecular clouds, where optical depths are high and the ambient radiation field of the galaxy is screened, temperatures are low ( $T < 50$  K). Under these conditions, most gas-phase species are quickly condensed onto the more refractory grains in the form of mixed-molecular ices (6). These ices contain a variety of molecular species, the most abundant of which is H<sub>2</sub>O (1, 7). Laboratory studies and astronomical observations have demonstrated that radiation processing of these ices modifies them and creates more complex molecular species (8).

Past laboratory photochemical studies of interstellar ice analogs have primarily been concerned with the irradiation of the most abundant simpler compounds known to be in the ices, such as H<sub>2</sub>O, CH<sub>3</sub>OH, NH<sub>3</sub>, CO, CO<sub>2</sub>, and H<sub>2</sub>CO (8). Only minimal consideration has been given to the presence of PAHs in these ices (9). Because PAHs represent a substantial portion of the interstellar carbon inventory,

~20% of the cosmically available carbon (3, 4), it is important to understand their behavior in the radiative processing of interstellar ices. The processing of PAHs in interstellar ices may also contribute to the materials incorporated into planets, satellites, asteroids, and comets. PAHs are present in meteorites (10, 11) and interplanetary dust particles (IDPs) (12, 13), have been observed in absorption toward young stellar objects (14), and were reported in Comet P/Halley (15).

We used IR spectroscopy and microprobe laser desorption laser ionization mass spectrometry ( $\mu\text{L}^2\text{MS}$ ) to study the photochemistry that occurs when PAHs are irradiated in H<sub>2</sub>O ices by ultraviolet (UV) light. The irradiation apparatus (16) consists of an evacuated sample chamber containing a rotatable 10 K CsI substrate coupled to a Fourier transform IR spectrometer (17). For the IR experiments, the PAH of interest and H<sub>2</sub>O were simultaneously vapor deposited onto the substrate. The H<sub>2</sub>O was deposited from a previously prepared glass sample bulb through a room-temperature sample inlet tube, whereas the PAHs were deposited from a separate, heated Pyrex sample tube. Analysis of IR band areas indicates that our sample layers typically had a thickness of 0.1  $\mu\text{m}$  and H<sub>2</sub>O/PAH ratios of 800 to 3200. After deposition, the IR spectrum of the PAH-H<sub>2</sub>O ice was measured at a resolution of 0.9  $\text{cm}^{-1}$ . The sample was then UV irradiated with a microwave-powered, flowing hydrogen, discharge lamp (18), which produces  $\sim 2 \times 10^{15}$  photons  $\text{cm}^{-2} \text{s}^{-1}$ , the flux being nearly evenly divided between the hydrogen Lyman  $\alpha$  line and a roughly 20-nm-wide molecular transition centered at 160 nm. Under such conditions, the time that elapses between photons arriving in the same molecular neighborhood is  $\sim 13$  or-

ders of magnitude longer than molecular relaxation times, so only one-photon processes are relevant. Typically, each layer was irradiated for a total of 200 min, although some experiments were carried out for  $>1000$  min. The loss of parent PAH and growth of product species during irradiation were monitored by measuring IR spectra of the sample at intervals of 5 to 30 min, depending on the half-life. When the irradiation was complete, the sample was slowly warmed to room temperature to gently sublime the H<sub>2</sub>O. A final IR spectrum was measured at room temperature.

For mass spectrometric analysis, samples were made in a similar fashion, except that the ice was formed on a 1-cm-diameter brass sample holder, the H<sub>2</sub>O and PAH being deposited and irradiated as before. Then the brass sample holder was removed and placed in the sample chamber of the microprobe laser desorption laser ionization mass spectrometer (10, 19, 20), and mass spectra were recorded of nonvolatile, PAH-related photo-products remaining on the sample holder.

To date, we have used IR spectroscopy to study the photochemical alteration rate of naphthalene (C<sub>10</sub>H<sub>8</sub>), anthracene (C<sub>14</sub>H<sub>10</sub>), phenanthrene (C<sub>14</sub>H<sub>10</sub>), tetracene (C<sub>18</sub>H<sub>12</sub>), chrysene (C<sub>18</sub>H<sub>12</sub>), pyrene (C<sub>16</sub>H<sub>10</sub>), pentacene (C<sub>22</sub>H<sub>14</sub>), perylene (C<sub>20</sub>H<sub>12</sub>), benzo(e)pyrene (C<sub>20</sub>H<sub>12</sub>), benzo[ghi]perylene (C<sub>22</sub>H<sub>12</sub>), and coronene (C<sub>24</sub>H<sub>12</sub>) in H<sub>2</sub>O ices. We also obtained IR spectra of the room-temperature residue produced when coronene is photolyzed in H<sub>2</sub>O ices. The  $\mu\text{L}^2\text{MS}$  technique was used to study the residues remaining after the photolysis and warm-up of pyrene-, benzo[ghi]perylene-, and coronene-containing samples.

PAH IR absorption band strengths are weak compared with those of H<sub>2</sub>O ice, and only their strongest bands, those corresponding to C–H out-of-plane bending modes, were typically detectable at 10 K. In all cases, these bands decreased exponentially with irradiation time, but the time scale varied substantially from PAH to PAH. The shortest “half-life” found was that of anthracene ( $\sim 50$  min) and the longest was that of naphthalene ( $\sim 500$  min). During irradiation, a weak broad absorption band also appeared spanning the 2950 to 2800  $\text{cm}^{-1}$  aliphatic C–H stretching region. Additional bands became apparent after warm-up to 300 K, and the results are summarized in Table 1. Particular attention is called to the presence of  $>\text{C}=\text{O}$  and  $-\text{O}-\text{H}$  (carbonyl and alcohol) functional groups. Preliminary IR spectra of the photolysis residues of several other PAH-H<sub>2</sub>O ice mixtures implicated the same classes of functional groups.

Turning now to the mass spectral data (Fig. 1), we see that unirradiated coronene produces a characteristic parent peak near 300 atomic mass units (amu) (and smaller peaks near 301 and 302 amu caused by the natural abundance of <sup>13</sup>C), whereas the spectrum of the residue

<sup>1</sup>NASA-Ames Research Center, Mail Stop 245-6, Moffett Field, CA 94035-1000, USA. <sup>2</sup>SETI Institute, 2035 Landings Drive, Mountain View, CA 94043, USA. <sup>3</sup>Department of Chemistry, Stanford University, Stanford, CA 94305-5080, USA.

\*To whom correspondence should be addressed. E-mail: mbernstein@mail.arc.nasa.gov

displays other peaks corresponding to different species. These peaks at 316, 332, and 348 amu are coronene molecules to which one, two, or three oxygen atoms, respectively, have been added. The addition of two hydrogen atoms is also apparent for the two- and three-oxygen variants (Fig. 1). The IR and mass spectra of the other PAHs we studied show similar effects to varying degrees. For example, although the mass spectrum of the coronene residue shows up to three added oxygen atoms, mass spectra of residues from benzo[ghi]perylene (Fig. 2) and pyrene (not shown in Fig. 2) indicate the addition of only one oxygen atom. Benzo[ghi]perylene and pyrene add two hydrogen atoms, not only to the one-oxygen variant but also to the original PAH. In all cases, the amount of material converted during 200 min of photolysis is no more than 20% and more typically only about 5%.

The ketone should be in equilibrium with an aromatic alcohol form by keto-enol tautomerism. The presence of a ketone is demonstrated by the strong  $>C=O$  stretching band at  $1665\text{ cm}^{-1}$ . Although an alcohol is consistent with

the broad OH stretch near  $3350\text{ cm}^{-1}$ , it is not proven because this OH stretch is also consistent with  $H_2O$  trapped in the residue. To test for the presence of alcohols, we derivatized the residue of a coronene- $H_2O$  photolysis experiment with bis(trimethylsilyl)acetamide, an agent that reacts with alcohols but not ketones. Derivatization produced mass peaks at 388 and 476 amu, which establish the presence of mono- and di-alcohols. The nature of the  $\mu\text{L}^2\text{MS}$  technique and the uncertain equilibrium between the ketone and phenol forms preclude an accurate assessment of the relative amounts of alcohol and ketone forms.

The photolysis of benzo[ghi]perylene, which has a "bay region" in its periphery (see Figs. 2 and 3), showed evidence for another reaction process. Here, in addition to the types of products seen for coronene, there is also evidence for the addition of an oxygen atom with the simultaneous loss of two hydrogen atoms (Figs. 2 and 3), which indicates the formation of a bridging ether across the bay region of this PAH. This identification is consistent with the IR spectrum of this residue, which

contains an absorption band near  $1095\text{ cm}^{-1}$ , a feature indicative of a C-O single bond such as those of an aromatic ether or alcohol.

Extensive hydrogen exchange between the PAHs and the water matrix was demonstrated by the photolysis of coronene in  $D_2O$  ices (Fig. 4) and perdeuterated coronene ( $C_{24}D_{12}$ ) in  $H_2O$  ices. The degree of exchange indicates that the H atoms on the PAHs are labile under photolysis. The exchange occurs to a greater degree (8 to 15% for exchange of one to four D atoms) on PAHs to which an oxygen atom has added, suggesting that the H atoms on oxygenated rings are more labile than those on normal aromatic peripheral rings.

PAH photolysis in  $H_2O$  ices causes reduction, which yields partially hydrogenated aromatic hydrocarbons ( $H_n$ -PAHs) (21), and oxidation, producing ketones, or alcohols, and bridging ethers when bay regions exist in the parent PAH (see Fig. 3). In addition, hydrogen and deuterium atoms exchange readily between the PAHs and the ice. These alteration processes have different effects on the chemical nature of the material. Hydrogen atom addition transforms some of the peripheral rings into cyclic aliphatic hydrocarbon structures, thereby creating molecules with aromatic and aliphatic character and decreasing the overall degree of aromaticity. Ketone formation also disturbs the aromaticity of the original molecule, but ether and alcohol production does not. We see no evidence, at these fluences, for breaking of the PAH carbon skeleton or for photodimerization of the PAHs at this concentration. The aromatic alcohol is reminiscent of an intermediate postulated in a previous coronene- $H_2O$  study (9).

**Table 1.** IR spectral features observed at 300 K and functional group assignments.

IR spectral feature	Implied functional group (33)
$3350\text{ cm}^{-1}$ (very broad: $3600$ to $2950\text{ cm}^{-1}$ )	O-H stretching (alcohol, $H_2O$ )
$2930$ and $2850\text{ cm}^{-1}$	C-H stretch of aliphatic $-CH_2-$ (methylene)
$1665\text{ cm}^{-1}$	C=O stretch of $C=C-C=O$ (conjugated ketone)
$1440\text{ cm}^{-1}$	$-CH_2-$ bending of $-CH_2-C=O$ or $H_n$ -PAH
$1325\text{ cm}^{-1}$ (broad: $1475$ to $1175\text{ cm}^{-1}$ )	$-CH_2-$ bending of $-CH_2-C=O$ or $H_n$ -PAH
$1350\text{ cm}^{-1}$	C-H or OH in-plane bend (aromatic alcohol)
$1240$ and $1090\text{ cm}^{-1}$	C-O-R stretches (aromatic)
$\sim 965$ and $810\text{ cm}^{-1}$	C-H out-of-plane bend (aromatic)

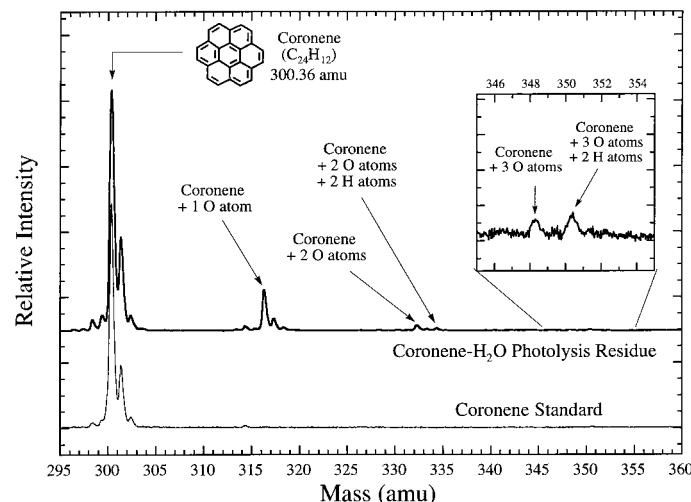
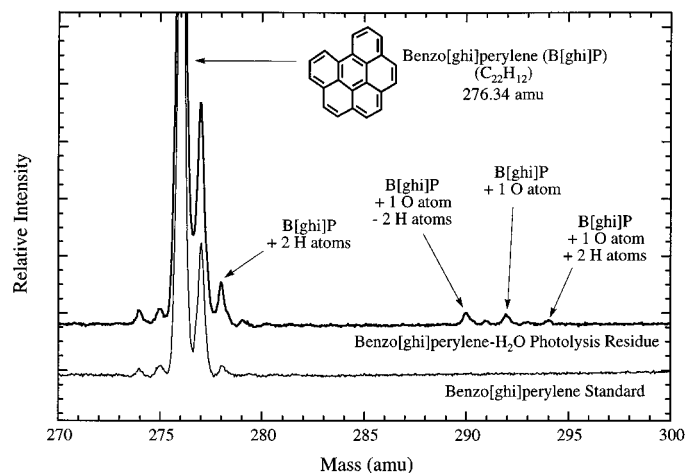


**Fig. 1 (left).** The  $\mu\text{L}^2\text{MS}$  spectrum of coronene ( $C_{24}H_{12}$ ) compared with that of a residue from a photolyzed coronene- $H_2O$  ice ( $H_2O/PAH > 800$ ). The peaks at 316, 332, and 348 amu correspond to the addition of one to three O atoms, respectively, likely in the form of ketones or hydroxyl side groups (or both). Elevated peaks at 334 and 350 amu (inset) indicate the addition of two H atoms to the doubly and triply oxygenated species. **Fig. 2 (right).** The  $\mu\text{L}^2\text{MS}$  spectrum of benzo[ghi]perylene ( $C_{22}H_{12}$ ) compared with that of a



residue from a photolyzed benzo[ghi]perylene- $H_2O$  ice ( $H_2O/PAH > 800$ ). The increase in the peak at 278 amu indicates the addition of two H atoms. The peak at 290 amu corresponds to the addition of an O atom with loss of two H atoms, consistent with an ether bridging the molecule's "bay" region. The peak at 292 amu corresponds to the addition of one O atom (as a ketone or hydroxyl group), and the peak at 294 amu corresponds to the addition of one O and two H atoms.

Although the specific reaction mechanism or mechanisms are not yet determined, we note that the disappearance rates of C–H out-of-plane bending modes can vary by a factor of 10, even for PAHs with similar peripheral structures (naphthalene compared with anthracene, for example). This observation rules out simple attack by H<sub>2</sub>O photofragments as the rate-determining step (22).

As PAHs are abundant throughout the interstellar medium, this work shows that the photochemistry of PAHs in interstellar ices is a potentially important contributor to the richness of interstellar organic chemistry. At the optical depth at which H<sub>2</sub>O ice becomes stable in dense interstellar clouds ( $A_v \approx 5$ ) (23), the 200-min exposure to our UV lamp corresponds to about 10<sup>5</sup> years. At optical depths of 10, the dosage corresponds to about 10<sup>7</sup> years, a time scale similar to the lifetime of a typical dense molecular cloud. Although UV fluxes deep in quiescent clouds will be lower, even there UV processing will occur as a result of background radiation induced by cosmic rays (24). The processes described here will be most important in UV-rich zones such as in the vicinity of protostars, where the observation of the 2165 cm<sup>-1</sup> band provides direct evidence for energetic processing (25). Thus, the UV photolysis of PAHs in interstellar ices should modify a portion of the interstellar PAH population in important ways. In particular, this process should transform PAHs into an ensemble of

organic compounds including polycyclic aliphatic hydrocarbons, H<sub>n</sub>-PAHs, aromatic ketones (quinones), aromatic alcohols, and aromatic ethers, all bearing some deuterium acquired from the ice.

The production of H<sub>n</sub>-PAHs is of particular interest because molecules of this type can account for important details in the IR emission spectra of a wide variety of interstellar objects. For example, IR features of H<sub>n</sub>-PAHs fit a number of weak emission features between 3080 and 2700 cm<sup>-1</sup> (3.25 to 3.7 μm) in the H I → H II transition region of the Orion Bar (21).

The addition of excess H atoms and photolytic hydrogen exchange may also bear on the deuterium enrichments of PAHs seen in meteorites (26) and in IDPs (13, 27). Interstellar ices are expected to be enriched in deuterium relative to cosmic abundances as the result of a number of low-temperature chemical processes (1, 28, 29). Given the apparent ease of hydrogen exchange between PAHs and water upon photolysis (Fig. 4), we would expect interstellar PAHs to become D enriched in dense clouds. This represents a different process for D enrichment of interstellar PAHs, in addition to the gas-phase unimolecular photodissociation mechanism proposed earlier (3, 12).

Other connections with the carbonaceous fractions of meteorites might also exist. Complex organic molecules similar to those produced here have been identified in meteorites

(10, 11), and oxidized PAHs are present in membrane-like boundary structures that form spontaneously from organic extracts from the Murchison meteorite (30). The formation histories of these materials are not well understood, although the presence of D enrichments in many of the classes of these compounds suggests an interstellar origin (26, 31). The photolytic processes discussed here may have contributed to the meteoritic inventory of deuterium-enriched PAHs.

Some of the molecules produced here are biologically interesting and therefore might contribute to establishing the primordial boundary conditions of the origin of life. For example, the species reported here include quinones (essential for electron transport in simple organisms) and aromatic alcohols that can partition into and modify the properties of lipid bilayer membranes. In other work, we have found that organic mixtures made in the multicomponent, realistic, interstellar ice analogs spontaneously form insoluble droplets when they are exposed to aqueous phases and selectively incorporate photoluminescent material (32). This observation of micellar type clustering akin to that seen for Murchison extracts, coupled with the results reported here, suggests that the inventory of organics that fell on early Earth was complex and should not be considered simply a source of reduced carbon for terrestrial processes to alter before incorporation into the first living organisms.

Fig. 3. The types of edge structures consistent with the IR and mass spectral data from the alteration products produced by the UV photolysis of PAH-H<sub>2</sub>O samples.

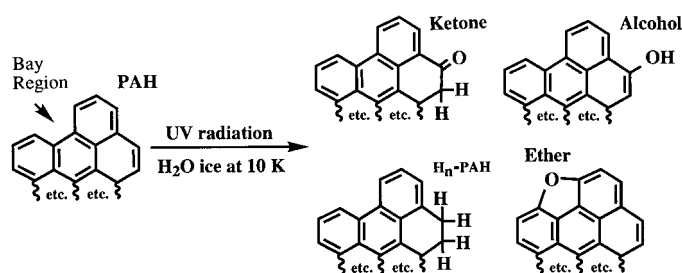
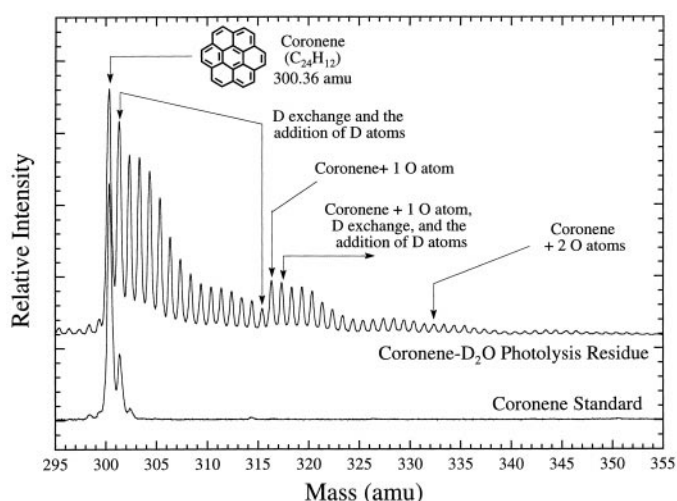


Fig. 4. The μL<sup>2</sup>MS spectrum of coronene (C<sub>24</sub>H<sub>12</sub>) compared with that of a residue from a photolyzed coronene-D<sub>2</sub>O ice (D<sub>2</sub>O/PAH > 800). In addition to the unreacted parent coronene (mass peak at 300 amu) and oxidized coronene (masses of 316 and possibly 332 and 348 amu), strong peaks are seen in the 301 to 315, 317 to 331, 333 to 347, and 349+ amu ranges, corresponding to deuterium exchange and addition to the original coronene and its oxidation products.



References and Notes

1. S. A. Sandford, *Meteoritic Planet. Sci.* **31**, 449 (1996).
2. W. M. Irvine, *Origins Life Evol. Biosphere* **28**, 365 (1998).
3. L. J. Allamandola, A. G. G. M. Tielens, J. R. Barker, *Astrophys. J. Suppl. Ser.* **71**, 733 (1989).
4. J. L. Puget and A. Leger, *Annu. Rev. Astron. Astrophys.* **27**, 161 (1989).
5. L. J. Allamandola, D. M. Hudgins, S. A. Sandford, *Astrophys. J. Lett.*, in press; F. Boulanger, P. Boissel, D. Cesarsky, C. Rytter, *Astron. Astrophys.* **339**, 194 (1998).
6. S. A. Sandford and L. J. Allamandola, *Astrophys. J.* **417**, 815 (1993).
7. A. G. G. M. Tielens et al., *ibid.* **287**, 697 (1984).
8. M. H. Moore, D. Bertram, R. Khanne, M. F. A'Hearn, *Icarus* **54**, 388 (1983); M. P. Bernstein, S. A. Sandford, L. J. Allamandola, S. Chang, M. A. Scharberg, *Astrophys. J.* **454**, 327 (1995); G. Strazzulla, A. C. Castorina, M. E. Palumbo, *Planet. Space Sci.* **43**, 1247 (1995); G. D. McDonald et al., *Icarus* **122**, 107 (1996); P. Gerakines, W. A. Schutte, P. Ehrenfreund, *Astron. Astrophys.* **312**, 289 (1996).
9. C. X. Mendoza-Gómez, M. S. de Groot, J. M. Greenberg, *Astron. Astrophys.* **295**, 479 (1995).
10. J. H. Hahn, R. Zenobi, J. L. Bada, R. N. Zare, *Science* **239**, 1523 (1988).
11. J. R. Cronin and S. Chang, in *The Chemistry of Life's Origins*, J. M. Greenberg, C. X. Mendoza-Gómez, V. Pirronello, Eds. (Kluwer Academic, Dordrecht, Netherlands, 1993), pp. 209–258, and references therein.
12. L. J. Allamandola, S. A. Sandford, B. Wopenka, *Science* **237**, 56 (1987).
13. S. Clemett, C. Maechling, R. Zare, P. Swan, R. Walker, *ibid.* **262**, 721 (1993).
14. K. Sellgren, T. Y. Brooke, R. G. Smith, T. R. Geballe, *Astrophys. J.* **449**, L69 (1995); T. Y. Brooke, K. Sellgren, R. G. Smith, *ibid.* **459**, 209 (1996); T. Y. Brooke, K. Sellgren, T. R. Geballe, *Astrophys. J. Suppl. Ser.*, in press.

15. G. Moreels, J. Clairemidi, P. Hermine, P. Brechignac, P. Rousselot, *Astron. Astrophys.* **282**, 643 (1994).
16. The irradiation apparatus is located at NASA's Ames Research Center.
17. D. M. Hudgins and L. J. Allamandola, *J. Phys. Chem.* **99**, 3033 (1995).
18. P. Warneck, *Appl. Opt.* **1**, 721 (1962).
19. The microprobe laser desorption laser ionization mass spectrometer is located at the Chemistry Department, Stanford University.
20. S. J. Clemett and R. N. Zare, in *Molecules in Astrophysics: Probes and Processes*, E. F. van Dishoeck, Ed. (International Astronomical Union, Dordrecht, Netherlands, 1997), pp. 305–320.
21. M. P. Bernstein, S. A. Sandford, L. J. Allamandola, *Astrophys. J.* **472**, L127 (1996); G. C. Sloan, J. D. Bregman, T. R. Geballe, L. J. Allamandola, C. E. Woodward, *ibid.* **474**, 735 (1996).
22. We propose a PAH cation intermediate in the oxidation and deuterium exchange reactions. Variations in the rate of disappearance of different PAHs would then be a consequence of efficiency of ionization of the neutral PAHs or stability of cation intermediates (or both).
23. D. C. B. Whittet *et al.*, *Mon. Not. R. Astron. Soc.* **233**, 321 (1988).
24. S. S. Prasad and S. P. Tarafdar, *Astrophys. J.* **267**, 603 (1983); A. Sternberg, A. Dalgarno, S. Lepp, *ibid.* **320**, 676 (1987).
25. S. C. Tegler *et al.*, *ibid.* **411**, 260 (1993).
26. J. F. Kerridge, S. Chang, R. Shipp, *Geochim. Cosmochim. Acta* **51**, 2527 (1987).
27. K. D. McKeegan, R. M. Walker, E. Zinner, *ibid.* **49**, 1971 (1985); S. Messenger *et al.*, *Meteoritics* **30**, 546 (1995); S. Messenger, R. M. Walker, S. J. Clemett, R. N. Zare, *Lunar Planet. Sci. Conf.* **XXVII**, 867 (1996).
28. A. G. G. M. Tielens, *Astron. Astrophys.* **119**, 177 (1983); in *Astrochemistry of Cosmic Phenomena*, P. D. Singh, Ed. (Kluwer, Dordrecht, Netherlands, 1992), pp. 91–95.
29. A. Dalgarno and S. Lepp, *Astrophys. J.* **287**, L47 (1984).
30. D. W. Deamer, *Microbiol. Mol. Biol. Rev.* **61**, 239 (1997).
31. J. R. Cronin, S. Pizzarello, S. Epstein, R. V. Krishnamurthy, *Geochim. Cosmochim. Acta* **57**, 4745 (1993).
32. L. J. Allamandola, M. P. Bernstein, S. A. Sandford, in *Astronomical and Biochemical Origins and the Search for Life in the Universe, Proceedings of the 5th International Conference on Bioastronomy, IAU Colloq. 161*, C. B. Cosmovici, S. Bowyer, D. Werthimer, Eds. (Editrice Compositori, Bologna, Italy, 1997), pp. 23–47.
33. A. S. Wexler, *Appl. Spectrosc. Rev.* **1**, 29 (1967).
34. Supported by NASA grants 344-37-44-01 (Origins of Solar Systems), 344-38-12-04 (Exobiology), NAG5-4936, and NAG5-7208. The authors are grateful for useful discussions with G. Cooper, J. Cronin, and D. Deamer and the excellent technical support provided by R. Walker. The authors would also like to thank the anonymous reviewers for helpful advice that improved the manuscript.

6 November 1998; accepted 12 January 1999

# Magma Flow Instability and Cyclic Activity at Soufriere Hills Volcano, Montserrat, British West Indies

**B. Voight,\*† R. S. J. Sparks, A. D. Miller, R. C. Stewart, R. P. Hoblitt, A. Clarke, J. Ewart, W. P. Aspinall, B. Baptie, E. S. Calder, P. Cole, T. H. Druitt, C. Hartford, R. A. Herd, P. Jackson, A. M. Lejeune, A. B. Lockhart, S. C. Loughlin, R. Luckett, L. Lynch, G. E. Norton, R. Robertson, I. M. Watson, R. Watts, S. R. Young**

Dome growth at the Soufriere Hills volcano (1996 to 1998) was frequently accompanied by repetitive cycles of earthquakes, ground deformation, degassing, and explosive eruptions. The cycles reflected unsteady conduit flow of volatile-charged magma resulting from gas exsolution, rheological stiffening, and pressurization. The cycles, over hours to days, initiated when degassed stiff magma retarded flow in the upper conduit. Conduit pressure built with gas exsolution, causing shallow seismicity and edifice inflation. Magma and gas were then expelled and the edifice deflated. The repeat time-scale is controlled by magma ascent rates, degassing, and microlite crystallization kinetics. Cyclic behavior allows short-term forecasting of timing, and of eruption style related to explosivity potential.

Growth of the andesite lava dome at Soufriere Hills volcano, Montserrat, has been unsteady and frequently accompanied by cyclic patterns of ground deformation, seismicity, pyroclastic flow generation, and explosive eruptions, overprinted on a background of continuous lava extrusion. We describe the

cycles, interpret the causes of cyclic behavior, and develop models for deformation and magma flow. Recognition of cyclic behavior enables short-term forecasting and improved management of volcanic crises. The cycles provide insights into eruption dynamics at andesite volcanoes, showing that degassing, rheological stiffening of the magma, and pressurization in the uppermost parts of volcanic conduits are intimately coupled and control many of the geophysical and dynamical phenomena observed.

The eruption of Soufriere Hills began on 18 July 1995 (1). Earthquake swarms and phreatic explosions preceded the extrusion of an andesite lava dome in mid-November 1995. Dome growth was accompanied by

rockfalls and dome collapses producing pyroclastic flows. Some substantial dome collapses were followed by explosive eruptions: a subplinian eruption on 17 September 1996 (2), and sequences of vulcanian explosions on 3 to 12 August and September to October 1997. Activity has been monitored by telemetered short-period and broadband seismic networks (3–5) (Fig. 1), electronic tilt stations as close as 150 m from the crater rim (6), global positioning system (GPS) and electronic distance measurement (EDM) methods (7, 8), correlation spectrometer measurements of SO<sub>2</sub> flux (9), visual observations, and surveys of dome and pyroclastic deposit volumes (10).

Seismic cycles have been recognized since 20 July 1996. Before this date, individual hybrid earthquakes had typically been repetitive, of similar size, and regular spacing, but the earthquake swarms showed no clear regularity (5). After this date, the earthquakes ceased to be repetitive, but the events were clustered in swarms. The period in November and early December 1996 was particularly instructive and was characterized by major deformation of the steep southern flank of the volcano known as the Galways Wall. Large fractures and seismically triggered landslides indicated that the Galways Wall was under severe stress. Edifice landslides could be distinguished seismically from dome rockfalls, and deformation of the Galways Wall correlated with hybrid swarms. Dome growth was more active in the aseismic periods.

Tilt cycles were first recognized in January 1997, when low-amplitude (~2 μrad) cyclic inflation and deflation with 6- to 8-hour periods were observed (6). Tilt cycles represent deformation of the volcanic edifice. More distinct rhythmic patterns (amplitude 15 to 20 μrad, period 12 to 18 hours) were observed in May 1997 (Fig. 2). Deflations are generally more rapid than inflations. In many individual cycles the edifice returned to near-

Montserrat Volcano Observatory, Montserrat, British West Indies.

\*To whom correspondence should be addressed at the Department of Geosciences, Penn State University, University Park, PA 16802, USA. E-mail: voight@ems.psu.edu

†Also affiliated with U.S. Geological Survey Volcano Hazards Program, Cascades Volcano Observatory, Vancouver, WA, and on Montserrat, with British Geological Survey.